Ionic Aggregation in a Block Copolymer Ionomer

Xinya Lu, W. P. Steckle, and R. A. Weiss*

Polymer Science Program and Department of Chemical Engineering, University of Connecticut, Storrs, Connecticut 06269-3136

Received February 26, 1993; Revised Manuscript Received August 9, 1993®

ABSTRACT: Small-angle X-ray scattering (SAXS) measurements of block copolymer ionomers based on lightly sulfonated poly(styrene-*b*-(ethylene-*co*-butylene)-*b*-styrene) (29.8% (by weight) styrene; M_n = 50 000) revealed a unique three-phase microstructure consisting of ionic aggregates dispersed within the polystyrene domains of the block copolymer. Compression-molded specimens exhibited an ellipsoidal microstructure with a domain diameter of ca. 11–13 nm, while a well-ordered lamellar microstructure with 6.5–7.5-nm lamella thickness resulted from solution casting. The ionic domain size was restricted by the size of the polystyrene domains in which they were dispersed. An ionic aggregate size of ca. 2 nm and a closest approach distance of ca. 3.5 nm were obtained from a modified hard-sphere, interparticle interference model for the ionic domains. The ionic domain size was insensitive to sulfonation level, but the aggregates for the Na salts were larger than for the corresponding Zn salts. The block domain spacing in a block ionomer with a lamellar microstructure was independent of sulfonation level, which suggests that polymer chain dimensions are unperturbed by the presence of ionic interactions. The critical temperature for ionic aggregate dissociation in the block copolymer ionomer was lower than that for similar homopolymer ionomers due to perturbation by the block microstructure. The critical temperature for disappearance of the ionic microstructure was 235–250 °C for the Zn salts; no ionic dissociation temperature was observed up to 300 °C for alkali-metal salts.

Introduction

Over the past 2 decades, there have been extensive experimental and theoretical studies directed at understanding the relationship between ion aggregation and the unique properties of ionomers.[1–10] The early studies considered random ionomers where the ionic groups are randomly placed along the polymer chain. This was followed by considerable activity with telechelic ionomers where the ionic groups are located at the chain ends. Those materials had the advantage from the perspective of theory in that the position of the ionic species on the chain was known. More recently, several groups have examined segmented ionomers[11,12] and block copolymer ionomers[13–16] where one of the segments or blocks is fully or partially ionized.

The most direct evidence for ionic aggregation in ionomers is a characteristic maximum or so-called *ionomer peak* observed by small-angle X-ray scattering (SAXS). The ionomer peak usually occurs at a scattering angle corresponding to a Bragg spacing of 2–6 nm. Although the SAXS of numerous ionomers is well documented, the origin of the ionomer peak is still unresolved, especially for random ionomers. Two general types of microstructural models have been proposed to quantitatively explain the SAXS patterns observed for ionomers: (1) *intra*particle interference models that attribute the ionomer peak to scattering within ionic aggregates[17,18] and (2) *inter*particle interference models that attribute it to scattering between ionic aggregates.[19] Because of the limited structure in the SAXS patterns, i.e., only a single, broad scattering maximum is usually observed for ionomers, and the many adjustable parameters involved in the models, quantitative interpretation of the SAXS data is neither straightforward nor universally agreed upon.

Some insight into the mechanism of ionic aggregation and the morphology of ionomers has been gained from studies of model ionomers. For example, SAXS studies of telechelic ionomers[20] indicated that the ionic groups aggregated into *multiplets* distributed with liquidlike order in the organic matrix, and an *inter*particle interference model provided the best agreement with the experimental data. Extension of that work to ionomers with variable-length side chains also indicated that the SAXS peak was due to *inter*particle interference.[21] Similar conclusions were also made from SAXS measurements of segmented ionomers.[22–24]

Studies of the model ionomers described above suggest that a similar microstructure with liquidlike order might also apply to random ionomer where the location of the ionic groups is randomly situated along the polymer chain. However, the experimental evidence for this has so far been inconclusive.

We recently reported the structure and properties of a block copolymer ionomer prepared by lightly sulfonating a poly(styrene-*b*-(ethylene-*co*-butylene)-*b*-styrene) (SEBS) triblock copolymer.[15,25,26] The lightly sulfonated polystyrene block is essentially a random ionomer, and a unique three-phase morphology consisting of ionic aggregates within the ordered microdomains of the block copolymer was observed for those materials. That novel morphology was the result of two separate levels of microphase separation, a 10–30-nm structure characteristic of the block copolymer and a 2–4-nm structure due to the salt groups.

The sulfonation process used to prepare sulfonated SEBS (S-SEBS) was the same as that used to make lightly sulfonated polystyrene ionomers (PS), which is an extensively studied random ionomer. The novel block-ionomer system may provide some insight into the ionic aggregation in a random ionomer. First, we expect that SPS and S-SEBS have similar distributions of the ionic groups along the polystyrene chain and similar ionic microstructures—the SAXS patterns corresponding to the ionic peak for the two polymers are indistinguishable. Second, the ionic aggregation in S-SEBS is restricted to within the ~10-nm block copolymer microdomains, and any microstructural model has to accommodate this fact. Third, the critical temperature for dissociation of the ionic aggregates is observable for the S-SEBS ionomers, presumably because the additional driving force for block mixing destabilizes the ionic aggregation within the

® Abstract published in *Advance ACS Abstracts*, October 1, 1993.

0024-9297/93/2226-5876$04.00/0

microdomains at elevated temperature. A critical temperature for dissociation of the ionic aggregates was predicted 2 decades ago by Eisenberg,[27] but it has not been observed experimentally for either random ionomers[28-31] or telechelic ionomers.[20] Finally, a preliminary SAXS study of solution-cast S-SEBS ionomers[32] indicated that they had a well-ordered lamellar microstructure. This may make it possible to assess the effect of ionic aggregation on the single-chain dimension of the ionomeric block from measurements of the thickness of the ionomeric block lamellae. Various conflicting theoretical predictions have been made for the effect of ionic aggregation on polymer chain dimensions,[33-36] and experimental results[37-42] have been largely inconclusive.

In the present study, the effects of sulfonation level, metal cation, and sample preparation on the block and ionic microstructures of S-SEBS ionomers were determined from synchrotron SAXS measurements. The SAXS results are discussed in the context of *intra*particle interference and *inter*particle interference models. Temperature-resolved SAXS measurements were also made to determine the critical temperature for dissociation of the ionic aggregates.

Experimental Section

Materials. Lightly sulfonated poly(styrene-*b*-(ethylene-*co*-butylene)-*b*-styrene) was prepared using acetyl sulfate as the sulfonating reagent according to the procedure described in a previous paper.[15] The starting SEBS polymer was obtained from Shell Development Co. and had a M_n = 50 000 and a composition of 29.8% (by weight) styrene. The sulfonation level of the polymer was determined by titration of S-SEBS in a mixed solvent of toluene/methanol (90/10, v/v) to a phenolphthalein endpoint. Sodium, zinc, and cesium salts of S-SEBS were prepared by neutralizing the free acid derivative in a toluene/methanol mixed solvent with the appropriate metal hydroxide or acetate. The nomenclature used for the samples was *x.y*M-S-SEBS, where *x.y* was the sulfonation level in mol % of the substituted styrene and M denoted the cation.

Polymer films for SAXS measurements were prepared by solution-casting and by compression-molding. The solvents used for the solution casting were toluene/dimethylformamide (DMF) mixtures varying from 2 to 10% (by volume) DMF, depending on the sulfonation level of the sample. The solvent was evaporated in air and the films were dried under vacuum for 2 days at 50 °C. The films were annealed for 2 h at 120 °C before the SAXS measurements.

SAXS Measurements. SAXS experiments were run at the Stanford Synchrotron Radiation laboratory (SSRL) using beamline I-4 and at the National Synchrotron Light Source (NSLS) at Brookhaven National Laboratories using the modified Kratky SAXS camera on beamline X3A2. The instruments are described elsewhere.[43,44]

At SSRL, two detectors were used, one placed immediately before and one after the specimen to monitor the beam decay and the sample absorption coefficient. The wavelength of the incident X-rays was λ = 0.143 nm. The sample was contained in an aluminum sample cell fabricated from a conventional DSC pan, and a Mettler FP82 hot stage was used to control the temperature. Because the characteristic size for the block microphase separation was much larger than that of the ionic microphase separation, two different sample to detector distances (SDD) were used. For the longer SDD the accessible scattering vector range was q = 0.06–1.2 nm^{-1}, where $q = 4\pi \sin(\theta/\lambda)$ and 2θ is the scattering angle; for the shorter SDD, q = 0.5–5 nm^{-1}. The two experimental geometries were used to characterize the block and ionic microphase separation, respectively. The data were corrected for dark current, detector homogeneity, parasitic and background scattering, and sample absorption.

At NSLS, λ = 0.154 nm. The sample was contained in an aluminum sample holder covered with a thin Kapton windows, and the sample assembly was fit into a custom-built temperature control apparatus.[45] The SDD was varied to yield q = 0.08–6.3 nm^{-1}. Two scintillation counters were placed before and after the sample to determine the decay of the incident beam and sample absorption coefficient.

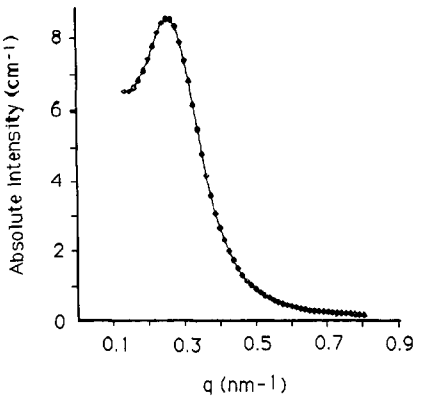

Figure 1. SAXS pattern for the block microstructure for compression-molded 12Zn-S-SEBS.

Table I. Morphological Parameters for Compression-Molded Block Copolymer Ionomers

sample	periodic length (nm)	domain size (nm)	core–shell model			modified hard-sphere model	
			R_1	R_2	R_3	R_1	$2R_{ca}$
3Zn-S-SEBS	26.2	13.1	1.26	4.5	5.3	1.09	4.52
5ZnS-SEBS	25.6	12.8	1.24	4.2	5.4	1.16	4.11
8.7Zn-S-SEBS	25.1	12.5	1.19	4.1	4.9	1.17	3.83
12Zn-S-SEBS	24.6	12.3	1.20	4.0	4.8	1.17	3.68
18Zn-S-SEBS	25.2	12.6	1.11	3.8	4.6	1.18	3.32
5Na-S-SEBS	26.0	13.0				1.25	4.18
8.7Na-S-SEBS	25.9	13.0				1.26	3.81
12Na-S-SEBS	25.7	12.9				1.25	3.46
18-NaSEBS						1.24	3.32

Results and Discussion

Block Copolymer Ionomer Structure. Compression-Molded Zn-S-SEBS. The SAXS data corresponding to the block microstructure for a compression-molded (CM) 12Zn-S-SEBS specimen are shown in Figure 1. The scattering profile exhibits a single peak centered at ca. q = 0.255 nm^{-1}, which corresponds to a microphase periodicity of 24.6 nm. It is not possible to unambiguously identify the block copolymer microstructure on the basis of Figure 1 alone, but transmission electron microscopy (TEM) of this material[26] indicated a dispersed microphase structure that is best described as deformed spheres with very diffuse phase boundaries. Based on the SAXS data, a rough estimate for the average phase size of a spherical, sulfonated polystyrene phase (hereafter, referred to as b-ZnSPS) with a face-centered-cubic arrangement is 12.3 nm, which is consistent with the value of 10–15 nm measured by TEM.[26]

The SAXS profiles for other compression-molded *x.y*Zn-S-SEBS block copolymer ionomers where *x.y* = 3–18 were similar to that of 12-Zn-S-SEBS, and the sizes for spherical microphases based on the SAXS data for those samples are listed in Table I. The phase periodicity and the phase size decreased slightly with increasing sulfonation level. The values in Table I were calculated from the position of the peak maximum, and the differences are probably due to an increase in the disorder of the microstructure as a consequence of the introduction of the sulfonate groups. That explanation is consistent with the more diffuse phase structure observed in TEM micrographs.[26]

Figure 2 shows SAXS data in the ionomer peak region for compression-molded Zn-S-SEBS as a function of the sulfonation level. All the curves exhibited a single, broad peak between $q \sim$ 1.3 and 1.8 nm^{-1}, which is the same

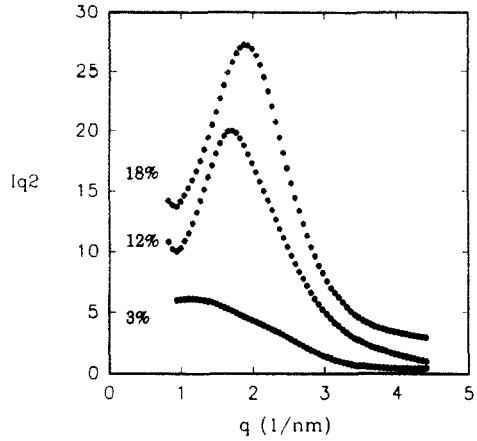

Figure 2. SAXS pattern for the ionic aggregation in compression-molded samples of ZnS-SEBS.

region where a similar SAXS peak is usually observed for SPS ionomers.[8] This *ionomer peak* is generally taken as evidence for ionic aggregation in ionomers, and for the Zn-S-SEBS polymers, it indicates that ionic aggregation occurs within the b-ZnSPS microdomains.

Two categories of microstructure models have been used to interpret ionomer SAXS data: (1) *intra*particle interference models and (2) *inter*particle interference models. The core–shell model[17] (Figure 3a) and the modified hard-sphere model[19] (Figure 3b) are representative of the two classes of ionomer microstructure models. The core–shell model (CSM) consists of a compact ionic aggregate surrounded by a nonionic hydrocarbon zone and a shell of ionic material with an electron density lower than the core aggregate. The ionic SAXS peak is attributed to interference between the core and the shell. Conversely, the modified hard-sphere model (MHSM) ascribes the ionomer peak to interference between ionic aggregates with a radius R_1 arranged with liquidlike order that have a distance of closest approach of $2R_{ca}$. The two models predict the structure factors given in eqs 1–4.[17,19]

core–shell model (CSM)

$$F(q) = \{(4\pi/3)\{\rho_1 R_1^3 \Phi(qR_1) + \rho_2[R_3^3 \Phi(qR_1) - R_2^3 \Phi(qR_1)]\}\}^2 \quad (1)$$

where

$$\Phi(x) = 3(\sin x - x \cos x)/x^3 \quad (2)$$

and R_1, R_2, and R_3 are the radii of the core, the nonionic hydrocarbon zone, and the shell, respectively. The position of the ionomer peak is associated with the radius of the shell, R_3 (see Figure 3a).

modified hard-sphere model (MHSM)

$$F(q) = V_1^2 \rho_1^2 \Phi(qR_1)/(1 + (8V_{ca}/V_p)\epsilon\Phi(2qR_{ca})) \quad (3)$$

where

$$V_{ca} = 4\pi R_{ca}^3/3; \qquad V_1 = 4\pi R_1^3/3 \quad (4)$$

Parts a and b of Figure 4 show the best fits of the SAXS data for 12Zn-S-SEBS by CSM and MHSM, respectively; the values for the adjustable parameters for both models are listed in Table I. The first item of particular interest is the ionic aggregate size. Since the ionic aggregation occurs within the b-ZnSPS microdomains, the aggregate size must be smaller than the microdomain size. Both

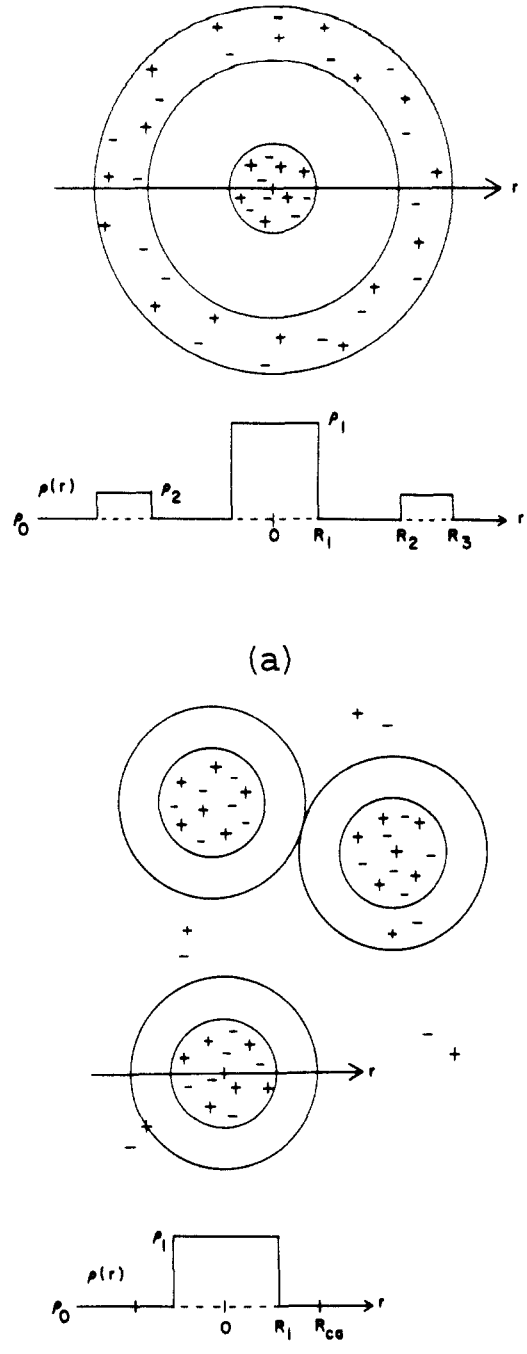

Figure 3. (a) Core–shell model of an ionic aggregate and its electron density profile. (b) Modified hard-sphere model and the corresponding electron density profile. (Reproduced from ref 19 with permission, copyright American Chemical Society.)

models adequately fit the ionic peak and yield aggregate parameters similar to the values obtained for SPS ionomers.[19] The models, however, differ in their prediction of the size of the ionic aggregates; the CSM consistently predicted an aggregate size, $2R_3$, that was about 4 times that predicted by the MHSM, $2R_1$. For example, for 8.7Zn-S-SEBS, the CSM gave an aggregate diameter of $2R_3$ = 9.6 nm, while the MHSM gave a value of $2R_1$ = 2.4 nm.

Schematic morphologies for the block ionomer microstructure based on the SAXS results and the two ionomer models discussed above are shown in Figure 5. Clearly, the picture corresponding to the CSM is less appealing, because it is difficult to imagine that a single ionic aggregate

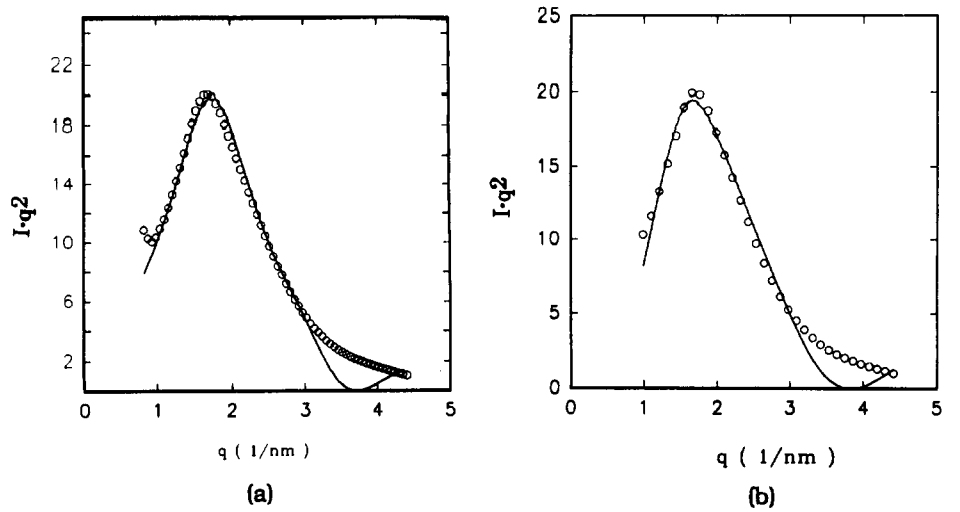

Figure 4. Comparison of the SAXS data for the ionic microstructure of compression-molded 12Zn-S-SEBS with (a) the core–shell model (R_1 = 1.2 nm, R_2 = 4.0 nm, and R_3 = 4.82 nm) and (b) the modified hard-sphere model (R_1 = 1.17 nm and R_2 = 3.68 nm) predictions. Solid curves represent the least-squares regressions of the models.

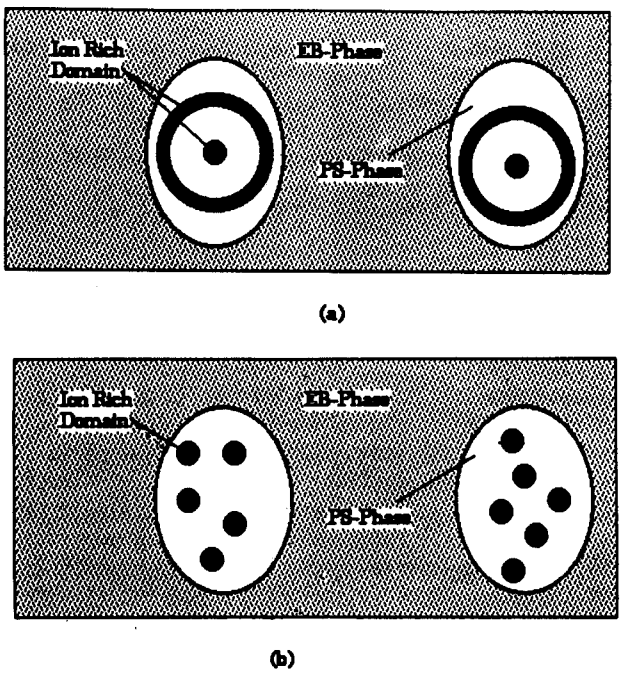

Figure 5. Schematic illustration of the microstructure of the compression-molded 12Zn-S-SEBS block copolymer ionomer corresponding to (a) a core–shell model ionic aggregate and (b) a modified hard-sphere model ionic aggregate. Structures are drawn to correspond to the block copolymer microstructure corresponding to the SAXS data in Figure 1 and the ionic microstructure model parameters calculated from the regressions in Figure 4.

could approach the size of the b-ZnSPS microdomain as shown in Figure 5a.

A glass transition of the b-ZnSPS domains was detected by DSC for all the polymers. The glass transition temperature, T_g, increased with increasing sulfonation level; the 18Zn-S-SEBS sample had a $T_g \sim 120$ °C. That glass transition is believed to be due to a polystyrene-rich phase, and the increase over that of a pure polystyrene phase (in the case of SEBS, $T_g \sim 80$ °C) is because association of the ionic groups, either as large microphase-separated aggregates or as small associated ion pairs (i.e., multiplets), restricts the mobility of the polymer chain. Although a second T_g for microphase-separated ionic aggregates is not observed by DSC for SPS ionomers, a relaxation that has been attributed to a *glass transition* for the ionic aggregates is detected by dynamic mechanical experiments. Following that reasoning, one must conclude that if the T_g of Zn-S-SEBS observed by DSC corresponds to the polystyrene phase, i.e., not the ionic aggregates, it phase size must be sufficiently large to be detected by calorimetry. That would seem to preclude the structure shown in Figure 5a, though the model shown by Figure 5b would be acceptable. In the latter case, a 2.4-nm-diameter ionic aggregate yields a figure of ca. 17–20 sulfonate groups/aggregate. If it is assumed that ~50% of the sulfonate groups were located in ionic aggregates,[19] space-filling calculations predict that, for 12Zn-S-SEBS, each b-ZnSPS microdomain contains ca. 20 ionic aggregates that occupy ca. 30% of the volume of the microdomain. A T_g of the ionic microphase was not resolved by DSC, which is consistent with a similar failure to detect an aggregate T_g in SPS ionomers by DSC.

The effect of sulfonate concentration on the ionic aggregate dimensions is also more easily explained with the liquidlike order structural model. The ionomer SAXS peak shifted to higher q with increasing sulfonation level. The MHSM indicated that when the sulfonation level increased from 3 to 5 mol %, the aggregate size (R_1) increased about 10% but then became independent of sulfonate concentration (see Table I). The closest approach distance ($2R_{ca}$), however, decreased monotonically with increasing sulfonate concentration which corresponds to an increase in the aggregate density within the microdomain. For instance, at low sulfonation levels, the local concentration of ionic groups available for aggregation inside the b-ZnSPS domain is relatively low. It is likely that the ionic groups first form smaller aggregates, which are enlarged when the sulfonation level increases. At some sulfonate concentration, ca. 5 mol % for Zn-S-SEBS, the aggregate size reaches a critical value determined by the steric hindrance of the polymer chain.[46] At that point, the size of the aggregates remains constant, but the number of aggregates within the microdomain increases.

Solution-Cast Zn-S-SEBS. It is well-known that sample history, and especially solvent effects, affect not only the extent of microphase separation in block copolymers but also the type of microstructure. Figure 6 shows SAXS data for the block microstructure of 5Zn-S-SEBS and 12Zn-S-SEBS samples cast from toluene/DMF mixed solvents. More structure was seen in the SAXS pattern of the solution-cast block copolymer ionomers than for the corresponding compression-molded samples (cf. Figures 1 and 6). At least three SAXS maxima were observed,

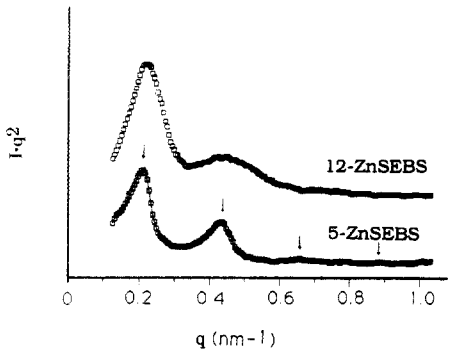

Figure 6. SAXS patterns for the block microstructure of 5Zn-S-SEBS and 12Zn-S-SEBS cast from toluene/DMF solutions (arrows denote scattering intensity maxima).

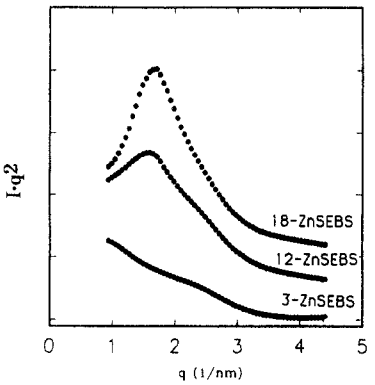

Figure 7. SAXS patterns for the ionic aggregation in Zn-S-SEBS block copolymer ionomers cast from toluene/DMF as function of the sulfonation level.

Table II. Morphological Parameters for Solution-Cast Zn-S-SEBS Block Copolymer Ionomers

sample	T (°C)	L (nm)	D (nm)	$\langle h_2 \rangle^{1/2}$ (nm)	CS model R_1	CS model R_2	CS model R_3	MHS model R_1	MHS model $2R_{ca}$
SEBS	50	7.3	28.1	6.1					
	250	6.9	26.6	5.8					
3Zn-S-SEBS	50	7.3	27.6	6.1					
	250	7.0	26.4	5.9					
5Zn-S-SEBS	50	7.4	27.4	6.2	1.24	4.4	5.4	1.11	4.40
	250	6.9	25.5	5.8					
12Zn-S-SEBS	50	7.1	26.3	5.9	1.18	4.1	5.0	1.20	3.95
	250	6.9	25.6	5.8					
18Zn-S-SEBS	50			1.15	3.9	4.9	1.19	3.6	

which indicate some long-range order in the spatial arrangement of the microdomains existed when the block copolymer ionomers were cast from solution. The ratio of q for the first-, second-, and third-order reflections was 1:2:3, which indicates a lamellar microstructure.

The first-order maximum is associated with the average nearest-neighbor distance, D, between the lamellar microdomains of b-ZnSPS given by Bragg's law:

$$D = 2\pi/q \tag{5}$$

The lamellar thickness, L, is calculated from the relation

$$L = DV_2 \tag{6}$$

where V_2 is the volume fraction of b-ZnSPS. The values of D and L calculated for the Zn-S-SEBS polymers are summarized in Table II.

The SAXS data of the ionic microstructure for the solution-cast samples are plotted in Figure 7. The solvent history also affected the ionic aggregation as evident by a less intense ionomer peak located at slightly lower q than for the corresponding compression-molded sample (cf. Figures 2 and 7). The effect was most significant at lower sulfonation levels, e.g., 3Zn-S-SEBS. Similar solvent effects were also observed for the ionic microstructure of SPS ionomers.[30]

The decrease of the ionomer peak intensity as a result of solution casting suggests a decrease in the ionic aggregate concentration. This is reasonable, because the solvent, especially a polar solvent like DMF, weakens or completely solvates the association between the ionic groups. The ionic aggregates cannot form until the polar cosolvent is removed. Depending on how the solvent is removed, it is conceivable that a nonequilibrium aggregate morphology is obtained, especially if the polar solvent is removed after the polymer on the microdomain vitrifies. In the case of SPS ionomers, Galambos et al.[30] demonstrated that one could even inhibit the formation of the ionic aggregates by a suitable solvent history for the sample. The interpretation for the shift of the ionomer peak to lower q is, again, model dependent. In the context of the liquidlike order model, that corresponds to an increase in the nearest-neighbor distance, $2R_{ca}$, which is a natural result of decreasing the aggregate concentration.

The least-squares parameters for the CSM and MHSM fits of the SAXS data in Figure 7 are listed in Table II. The lamellar b-ZnSPS microdomains of the solution-cast Zn-S-SEBS provide a clear test of the validity of the core–shell and modified hard-sphere models of the ionic aggregate structure in random ionomers. The CSM gave aggregate diameters of 8–10 nm for the Zn-S-SEBS, which is impossible given that the lamellar thickness of the b-ZnSPS was only 6–7 nm. This is shown schematically in Figure 8a.

The MHSM, however, provides a more acceptable ionic aggregate structure for the lamellar block copolymer ionomer microstructure. In that case, the ionic aggregate diameter was $2R_1 \sim 0.9$–1.0 nm and the center-to-center closest approach distance was 3–4 nm. Those dimensions are easily accommodated in a lamellar thickness of 6–7 nm for the b-ZnSPS microdomains (see Figure 8b). The model parameters cited here for the ionic microstructure of the block copolymer ionomers are comparable to those obtained for ZnSPS ionomers,[19,28] and it is tempting to assume that microstructures of both types of ionomers are similar.

For the solution-cast Zn-S-SEBS, the ionic aggregate size based on the MHSM, R_1, increased about 10% when the sulfonation level was increased from 5 to 12 mol %, but no further change occurred between 12 and 18 mol %. The average nearest-neighbor distance, R_{ca}, however, decreased with increasing sulfonation level over the entire range studied, 5–18 mol %. If the ionic aggregation is energetically favorable, the aggregate size should be determined by a balance between attractive forces for aggregation and the steric repulsion from of the backbone. The electrostatic attractive forces are associated with the ionic species and the steric hindrance is mainly dependent on the chain structure. As a result, the ionic aggregate size may vary with the ionomer type and the ionic species but should be relatively insensitive to the ionic concentration. The distance of closest approach of the aggregates should depend on the structure of the backbone chain, which affects the aggregate because the ionic group is covalently bound to the chain, and the concentration of the ionic groups. The latter variable controls the volume or the number density of aggregates. These concepts are consistent with the recent aggregate model proposed by Hird and Eisenberg.[46]

Compression-Molded Na-S-SEBS. Figure 9 shows SAXS data for the ionic microphase separation for 5Na-S-SEBS, 8.7Na-S-SEBS, and 18Na-S-SEBS. The effects

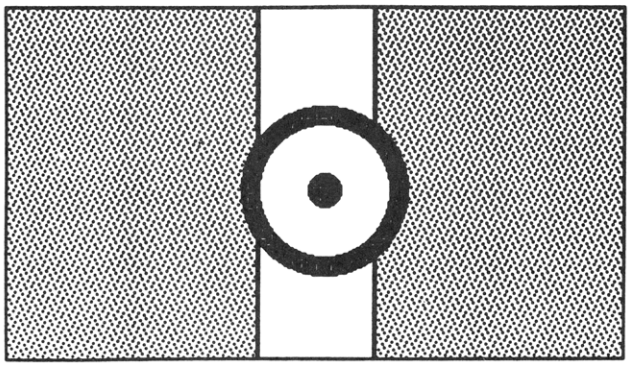

(a)

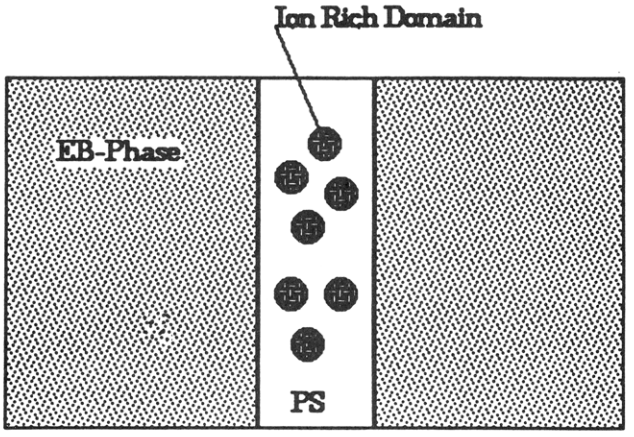

(b)

Figure 8. Schematic illustration of the microstructure of solution-cast 12Zn-S-SEBS corresponding to (a) the core–shell model and (b) the modified hard-sphere model. Structures are drawn to correspond to the block copolymer microstructure corresponding to the SAXS data in Figures 6 and 7.

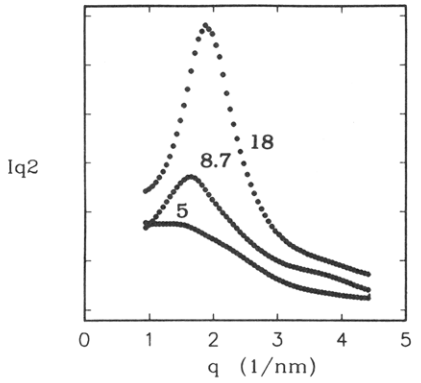

Figure 9. SAXS patterns for the ionic aggregation in compression-molded Na-S-SEBS block copolymer ionomers for various sulfonation levels.

of sulfonation were similar to that for the compression-molded Zn-S-SEBS. Increasing the sulfonation level led to two notable changes in the SAXS: (1) the peak position shifted from ca. 1.5 to ca. 1.85 nm^{-1} when the sulfonation level changed from 5 to 18 mol % and (2) the weak, broad peak for the lower sulfonation level developed into a sharp, intense peak at high sulfonation level. The peak shift to higher q corresponds to a decrease in the nearest-neighbor distance between the aggregates (assuming a MHSM). The sharpening of the peak and the increase in intensity indicates that the volume fraction of aggregates increased and the distribution of nearest-neighbor distances narrowed as the sulfonation level increased.

Structural parameters for the Na-S-SEBS obtained by fitting the SAXS data in Figure 9 with the MHSM are compared with the parameters for Zn-S-SEBS in Table I. The ionic aggregate size for the Na-S-SEBS ionomers was larger than for the Zn salts, but the closest approach distance for the aggregates was similar for the two salts. The larger aggregate size for the Na-S-SEBS may reflect better packing of the Na sulfonate groups or stronger ion-dipole interactions. The closest approach distance is a function of the nature of the backbone chain and the distribution of the ionic species on the chain. Because the different ionomers were prepared from the same *parent* sulfonic acid derivative, it is not surprising that little difference in R_{ca} was observed when the cation was changed.

Effect of the Ionic Interactions on the Chain Dimensions. An unresolved question for ionomers is what effect ionic association has on the chain conformation. Some theories predict chain expansion,[33–35] while another theory predicts that the chain dimension will be unperturbed from that of the unionized polymer.[36] Experiments have tended to support the expansion theories, but the results have not been conclusive. Two different experimental approaches to this problem have been used. One was to directly measure the radius of gyration, $\langle R_g \rangle$, of an ionomer chain by small-angle neutron scattering (SANS)[37–41] the other method was to measure the inter-aggregate spacing in a telechelic ionomer[20] or a segmented ionomer[42] by SAXS.

The lamellar microstructure of the solution-cast Zn-S-SEBS block copolymer ionomers offers another strategy for determining the effect of ionic interactions on polymer chain dimensions. Specifically, the lamellar thickness, L, defined in eqs 5 and 6, is related to the chain dimension of the block[47] by

$$L = k\langle h_A^2 \rangle^{0.5} \tag{7}$$

where $\langle h_A^2 \rangle^{0.5}$ is the mean-square end-to-end distance of block A, and k is a factor related to the block copolymer architecture ($k = 1.2$ for an ABA block copolymer[47]). The values of L for the starting SEBS and the Zn-S-SEBS ionomers can be determined from the SAXS data and eqs 5 and 6, and $\langle h_{PS}^2 \rangle^{0.5}$ and $\langle h_{ZnSPS}^2 \rangle^{0.5}$ can be calculated from eq 7. The calculated values for Zn-S-SEBS as a function of the sulfonation level and temperature are given in Table II.

For the neat SEBS, $\langle h_{PS}^2 \rangle^{0.5}$ for the polystyrene block can also be calculated from the block molecular weight, M_{ps},

$$\langle h_{PS}^2 \rangle^{0.5} = C_{ps} M_{ps}^{0.5} \tag{8}$$

For $C_{ps} = 0.0695$ nm,[48] $\langle h_{PS}^2 \rangle^{0.5} = 6.02$ nm for a polystyrene block having $M_{ps} = 7500$. This value agrees very well with the value of $\langle h_{PS}^2 \rangle^{0.5} = 6.1$ nm estimated from eq 7 using the lamellar thickness of $L = 7.3$ nm determined by SAXS.

The calculations for $\langle h_{ZnSPS}^2 \rangle^{0.5}$ for the Zn-S-SEBS ionomers at 50 °C given in Table II indicate that the block chain dimension is independent of sulfonation level up to 12 mol %. This result conflicts with the chain expansion theories[34,35] that predict as much as a 60% expansion of the chain for a sulfonation level of 12 mol %, but it agrees with the theory of Squires et al.[36] and a recent SANS study[41] that found no chain expansion due to ionic aggregation in a sulfonated polyurethane ionomer.

Limited data of the effect of temperature on $\langle h_{ZnSPS}^2 \rangle^{0.5}$ are also given in Table II. The chain size at 250 °C was slightly less than that at 50 °C, but, again, there was no effect of sulfonation on $\langle h_{PS}^2 \rangle^{0.5}$.

Dissociation Temperature of the Ionic Aggregates. In his seminal paper on the structure of ionomers, Eisenberg[27] proposed that the formation of the ionic aggregates involved a competition between dipole–dipole interactions that promote ionic aggregation and elastic forces that oppose ionic aggregation. In accordance with rubber elasticity theory, the elastic force increases with temperature, while the dipole–dipole interactions should be relatively insensitive to temperature. The Eisenberg theory predicts that a critical temperature for dissociation of the ionic aggregates occurs when the elastic forces exceed the magnitude of the dipole–dipole interactions.

The ionic aggregate microstructure at elevated temperatures has been investigated with SAXS for a variety of ionomers, including SPS ionomers,[28-30] poly(ethylene-*co*-*r*-methacrylic acid) ionomers,[28] and telechelic ionomers.[20] In each study, the ionic aggregates were found to be so stable that the polymer degraded before their dissociation could be observed.

The ionic aggregate dissociation was, however, observed with the Zn-S-SEBS block copolymer ionomers. One possible reason for the lower dissociation temperature for the ionic aggregates in the b-ZnSPS microdomains, compared with the Zn-SPS ionomers, is that, in addition to the elastic force of ionomer chain opposing the associated structure, there is also a force arising from a tendency for the blocks to mix that should destabilize ionic aggregation within the polystyrene microdomain. Like the elastic force, that additional force becomes more dominant at elevated temperature. As a result, the net force opposing the aggregate structure exceeds the associative forces at a lower temperature for the block copolymer ionomer than in the corresponding homopolymer ionomer.

Temperature-resolved SAXS measurements were made for Zn-S-SEBS and Cs-S-SEBS. Those salts were chosen, because a previous study[29] showed that the effects of temperature on the ionic aggregation of SPS ionomers were considerably different for an alkali-metal salt, i.e., a Na salt, and a Zn salt. Increasing temperature promoted phase mixing in Zn-SPS but increased phase separation in Na-SPS. That result indicated that the ionic associations for the alkali-metal salts of SPS are more thermally stable than those for the Zn salt, though complete dissociation of the ionic aggregates was not observed in either material.

Normalized SAXS data for the ionic microstructure of compression-molded 8.7Zn-S-SEBS collected while heating from 90 to 250 °C are shown in Figure 10. The SAXS patterns for $T \leq 90$ °C exhibited a broad peak characteristic of the ionic aggregation at $q \sim 1.42$ nm^{-1} and a strong upturn of the intensity at low q that may be due in part to an upturn usually observed in the SAXS of ionomers at low q or to the scattering from the larger block microphase. As the temperature was increased, the ionomer peak weakened and completely disappeared at 250 °C. The disappearance of the peak was also accompanied by an increase in the intensity at low q. Thus, it appears that 250 °C was the dissociation temperature for the ionic aggregates in that block copolymer ionomer.

Between the glass transition temperature of the b-ZnSPS at ca. 105 °C and the aggregate dissociation temperature of 250 °C, the ionomer peak broadens and becomes less intense, but the peak position remains constant. This indicates that some dissolution of the ionic material into the polystyrene-rich domains occurred,

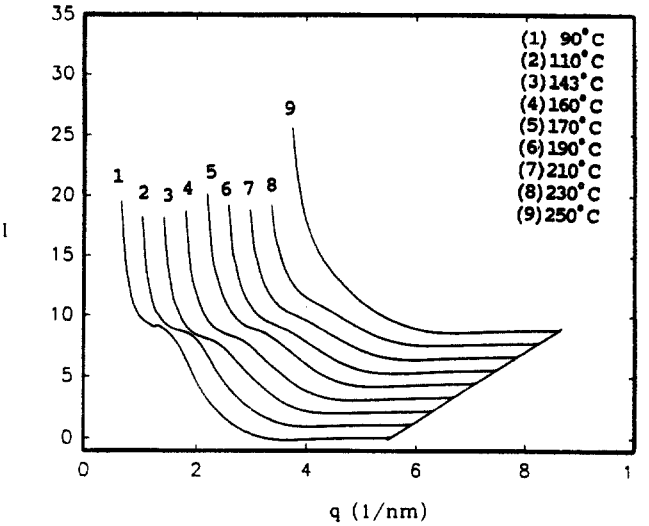

Figure 10. Temperature-resolved SAXS patterns for the ionic microstructure of compression-molded 8.7Zn-S-SEBS during a heating scan from 90 to 250 °C.

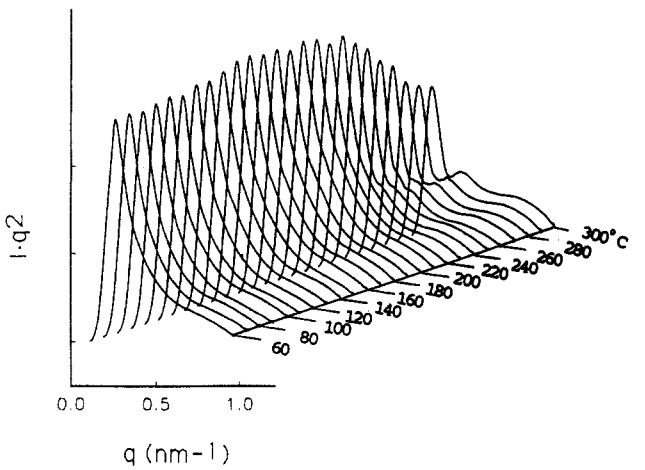

Figure 11. Temperature-resolved SAXS patterns for the block microstructure of compression-molded 8.7Zn-S-SEBS during a heating scan from 60 to 300 °C.

similar to what was observed at elevated temperature for Zn-SPS ionomers. For the latter materials, however, the ionomer peak persisted up to at least 300 °C.[28,29]

A transition of the block copolymer microstructure for 8.7Zn-S-SEBS from a spherical to lamellar geometry also occurred at 250 °C (Figure 11). That result confirmed that the forces controlling the order or disorder of the ionic aggregates and the block microstructure are coupled for these materials, and this probably explains the decrease in the ionic aggregate dissociation temperature for the block copolymer ionomers compared with Zn-SPS ionomers.

The ionic dissociation temperature for the Zn-S-SEBS ionomers was relatively insensitive to the sulfonation level. At relatively low sulfonation level, e.g., 3-Zn-S-SEBS, the dissociation temperature was ~235 °C, while the ionic dissociation temperature for two samples with higher sulfonation levels, 8.7-Zn-S-SEBS and 12-Zn-S-SEBS, were ~250 °C. The theory of Datye and Taylor[49] predicts that the ionic dissociation temperature is primarily governed by the aggregate size, which suggests that the ionic aggregate size in all the Zn-S-SEBS ionomers should be similar—that is, independent of sulfonation level. Because it neglects the effects of the polymer chain, the Datye and Taylor theory is inadequate for predicting the actual dissociation temperature of the aggregates, but its prediction of the invariance of the aggregate size with ionic

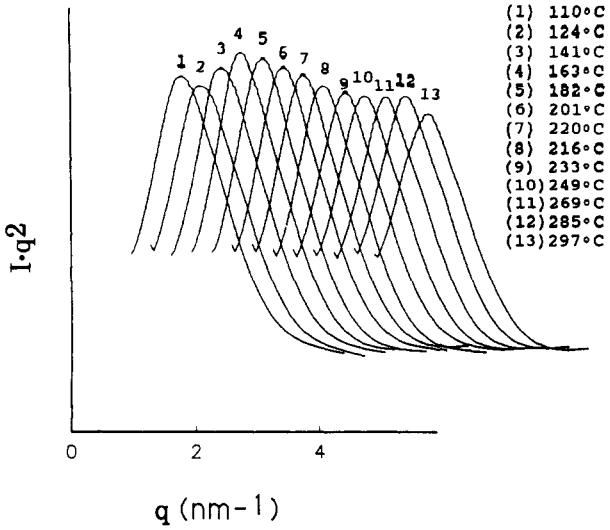

Figure 12. Temperature-resolved SAXS patterns for the ionic microstructure of compression-molded 12Cs-S-SEBS during a heating scan from 110 to 300 °C. (Each successive curve has been shifted along the q-axis by 0.33 nm^{-1}.)

concentration is consistent with the observation of Yarusso and Cooper for Zn-SPS ionomers.[28]

The compression-molded 12Cs-S-SEBS had a more thermally stable ionic microstructure. Figure 12 shows the SAXS curves during heating of this material from 110 to 300 °C. No ionic dissociation temperature was observed up to 300 °C. As the temperature was increased, the intensity of the ionomer peak first increased between ca. 110 and 163 °C but then decreased between 163 and 300 °C. This behavior was similar to that for Na-SPS.[29] The initial increase in the ionomer peak intensity was probably a result of improved chain mobility above T_g that allowed more ionic groups to participate in the aggregate structure. At higher temperatures, however, some phase mixing takes place that lowers the peak intensity, but nowhere near what occurs for the Zn-S-SEBS ionomers. For the Cs-S-SEBS, the onset of phase mixing occurred at ca. 165 °C, which was considerably lower than that for Na-SPS, for which no decrease in the ionomer peak intensity or the scattering invariant was observed until ~270 °C.[29] That result indicates that the ionic structure was weaker for Cs-S-SEBS than for Na-SPS, though both were much stronger than that for Zn-S-SEBS. The weaker aggregates in Cs-S-SEBS vis-à-vis Na-SPS may be due to the effect of the block copolymer microstructure as discussed earlier and/or the weaker dipole–dipole interactions between metal sulfonate groups for the Cs sulfonate groups compared with Na sulfonate.

When the differences in the aggregate structure of the Cs and Zn salts of S-SEBS are examined, it is not surprising that the alkali-metal salt has a higher dissociation temperature than the Zn salt. The alkali-metal salts have larger ionic aggregates that contain more ionic dipoles than the Zn salts as indicated by the model calculations for the S-SEBS ionomers (see Table I), as well as for SPS ionomers[28] and telechelic ionomers.[20] Morever, the alkali-metal salts may have tighter packing of the ionic species in the aggregate and stronger interactions between the ion pairs as proposed by Lefelar and Weiss.[50] Since both salts for a given ionomer have similar steric restrictions to aggregation, formation of a larger aggregate requires stronger dipole–dipole interactions. It follows that stronger dipolar forces will yield larger ionic aggregates, which in turn, will have higher dissociation temperatures.

Conclusions. The sulfonated SEBS ionomers exhibit a unique three-phase microstructure that consists of ionic aggregates dispersed within the microdomains of the sulfonated polystyrene blocks (b-SPS). Consideration of the b-SPS as a model ionomer has provided considerable insight into the mechanism of ionic aggregation and the microstructure of random ionomers.

The morphology of the b-SPS microdomains varied with sample preparation. Compression molding yielded an ellipsoidal microstructure with a domain diameter of ~11–13 nm, while a well-ordered lamellar microstructure with a lamellar thickness of 6.5–7.5 nm was observed for solution-cast samples. The ionic aggregation within the b-SPS microdomains exhibited SAXS patterns similar to those observed for SPS homopolymer ionomers. For the S-SEBS ionomers, the ionic aggregate size is restricted by the size of the b-SPS domains in which they are contained. As a result, structural model fits of SAXS data eliminated the possibility that the SAXS ionomer peak arises from intraparticle interference, because the sizes of the ionic aggregates predicted by these models, 8–10-nm diameter, are too large to fit into the b-SPS microstructure. A more reasonable aggregate size, ~2 nm, and a closest approach distance of ~3.5 nm were obtained from a modified hard-sphere, interparticle interference model.

For both the molded and solution-cast samples, the ionomer peak shifted to higher q as the sulfonation level increased, which indicates an increase in the volume of ionic aggregate. The ionic aggregate size, however, was relatively insensitive to sulfonation level but dependent upon the choice of the counterion. Na salts gave larger ionic aggregates than the corresponding Zn salts.

The restriction of the ionic aggregates to the b-SPS microdomains was utilized to determine the effect of ionic aggregation on the chain dimensions of a random ionomer. The interdomain spacing of a lamellar b-SPS microstructure was independent of sulfonation level, which indicated that the dimensions of the chain were unperturbed by the presence of the ionic interactions. This invariance of the chain dimensions with ionic content was consistent with at least one theoretical prediction[36] and recent SANS experiments[41] of another ionomer.

A critical temperature for ionic aggregate dissociation was observed between 235 and 250 °C for the Zn-S-SEBS ionomers, and it was relatively insensitive to the sulfonation level. The latter result further suggested that the ionic aggregate size is independent of the sulfonation level. For Cs-S-SEBS ionomers, the ionic aggregates were more thermally stable; no ionic dissociation temperature was observed up to 300 °C. The difference between the Cs and Zn salts is believed to be due to stronger dipole attraction in the ionic aggregates of the Cs-S-SEBS ionomers, which also yielded a larger ionic aggregate size.

Acknowledgment. This work was supported by the Office of Naval Research (Grant No. ONR N00014-91-J-1565).

References and Notes

(1) Eisenberg, A.; King, M. *Ion-Containing Polymers, Physical Properties and Structure*; Academic Press: New York, 1977.
(2) MacKnight, W.; Earnest, T. *J. Polym. Sci., Macromol. Rev.* **1981**, *16*, 41.
(3) Wilson, A. D., Prosser, H. J., Eds. *Developments in Ionic Polymers-1&2*; Applied Science Publishers: New York, 1983.
(4) Eisenberg, A., Bailey, F., Eds. *Coulombic Interactions in Macromolecular Systems*; ACS Symposium Series 302; American Chemical Society: Washington, DC, 1986.
(5) Pineri, M., Eisenberg, A., Eds. *Structure and Properties of Ionomers*; Reidel Publishing Co.: Dordrecht, Holland, 1987.
(6) Tant, M. R.; Wilkes, G. L. *J. Macromol. Sci., Rev.* **1988**, *C28*, 1.
(7) Mauritz, K. A. *J. Macromol. Sci., Rev.* **1988**, *C28*, 65.

(8) Fitzgerald, J. J.; Weiss, R. A. *J. Macromol. Sci., Rev.* **1988**, *C28*, 99.
(9) Utracki, L. A., Weiss, R. A., Eds. *Multiphase Polymers: Blends and Ionomers*; ACS Symposium Series 395; American Chemical Society: Washington, DC, 1989.
(10) Lantman, C. W.; MacKnight, W. J.; Lundberg, R. D. In *Comprehensive Polymer Science*; Allen, G., Bevington, J. C., Eds.; Pergamon Press: Oxford, U.K., 1989; Vol. 2, Chapter 25.
(11) Visser, S. A.; Cooper, S. L. *Macromolecules* **1991**, *24*, 2576.
(12) Feng, D.; Venkateshwaran, L. N.; Wilkes, G. L.; Stark, J. E.; Leir, C. M. *J. Appl. Polym. Sci.* **1989**, *37*, 1549.
(13) Gauthier, S.; Eisenberg, A. *Macromolecules* **1987**, *20*, 760.
(14) Long, T. E.; Allen, R. D.; McGrath, J. E. In *Chemical Reactions on Polymer*; Benham, J. L.; Kinstle, J., Eds.; American Chemical Society: Washington, DC, 1988.
(15) Weiss, R. A.; Sen, A.; Pottick, L. A.; Willis, C. L. *Polym. Commun.* **1990**, *31*, 220.
(16) Venkateshwaran, L. N.; York, G. A.; DePorter, C. D.; McGrath, J. E.; Wilkes, G. L. *Polymer* **1992**, *33*, 2277.
(17) MacKnight, W. J.; Taggart, W. P.; Stein, R. S. *J. Polym. Sci., Polym. Symp.* **1974**, *45*, 113.
(18) Fujimura, M.; Hashimoto, T.; Kawai, H. *Macromolecules* **1982**, *15*, 136.
(19) Yarusso, D. J.; Cooper, S. L. *Macromolecules* **1983**, *16*, 1871.
(20) Williams, C. E.; Russell, T. P.; Jérôme, R.; Horrion, J. *Macromolecules* **1986**, *19*, 2877.
(21) Moore, R. B.; Bittencourt, D.; Gauthier, M.; Williams, C. E.; Eisenberg, A. *Macromolecules* **1991**, *24*, 1376.
(22) Feng, D.; Wilkes, G. L.; Leir, C. M.; Stark, J. E. *J. Macromol. Sci., Chem.* **1989**, *26*, 1151.
(23) Visser, S. A.; Cooper, S. L. *Macromolecules* **1991**, *24*, 2584.
(24) Gouin, J.-P.; Williams, C. E.; Eisenberg, A. *Macromolecules* **1989**, *22*, 4573.
(25) Weiss, R. A.; Sen, A.; Pottick, L. A.; Willis, C. L. *Polymer* **1991**, *32*, 1867.
(26) Weiss, R. A.; Sen, A.; Pottick, L. A.; Willis, C. L. *Polymer* **1991**, *32*, 2785.
(27) Eisenberg, A. *Macromolecules* **1970**, *3*, 147.
(28) Yarusso, D. J.; Cooper, S. L. *Polymer* **1985**, *26*, 371.
(29) Weiss, R. A.; Lefelar, J. A. *Polymer* **1986**, *27*, 3.
(30) Galambos, A. F.; Stockton, W. B.; Koberstein, J. T.; Sen, A.; Weiss, R. A.; Russell, T. P. *Macromolecules* **1987**, *20*, 3094.
(31) Chu, B.; Wu, D.-Q.; MacKnight, W. J.; Wu, C.; Phillips, J. C.; LeGrand, A.; Lantman, C. W.; Lundberg, R. D. *Macromolecules* **1988**, *21*, 523.
(32) Steckle, W. P., Jr.; Lu, X.; Weiss, R. A. *Polym. Mater. Sci. Eng.* **1991**, *62* (2), 239.
(33) Forsman, W. C. *Macromolecules* **1982**, *15*, 1032.
(34) Forsman, W. C.; MacKnight, W. J.; Higgins, J. S. *Macromolecules* **1984**, *17*, 490.
(35) Dreyfus, B. *Macromolecules* **1985**, *18*, 284.
(36) Squires, E.; Painter, P.; Howe, S. *Macromolecules* **1987**, *20*, 1740.
(37) Pineri, M.; Duplessix, R.; Gauthier, S.; Eisenberg, A. *Adv. Chem. Ser.* **1980**, *187*, 283.
(38) Earnest, T. R.; Higgins, J. S.; Handlin, D. L.; MacKnight, W. J. *Macromolecules* **1981**, *14*, 192.
(39) Register, R. A.; Cooper, S. L.; Thiyagarajan, P.; Chakrapani, S.; Jérôme, R. *Macromolecules* **1990**, *23*, 2978.
(40) Register, R. A.; Pruckmayr, G.; Cooper, S. L. *Macromolecules* **1990**, *23*, 3023.
(41) Visser, S. A.; Pruckmayr, G.; Cooper, S. L. *Macromolecules* **1991**, *24*, 6769.
(42) Feng, D.; Wilkes, G. L. *Macromolecules* **1991**, *24*, 6786.
(43) Stephenson, G. B. Ph.D. Dissertation, Stanford University, Stanford, CA, 1982.
(44) Chu, B.; Wu, D. Q.; Wu, C. *Rev. Sci. Instrum.* **1987**, *58*, 1158.
(45) Hsaio, B.; Gardner, K. H.; Wu, D. Q.; Liang, B.; Chu, B. *Polym. Prepr. (Am. Chem. Soc., Div. Polym. Chem.)* **1992**, *33* (1), 265.
(46) Hird, B.; Eisenberg, A. *Macromolecules* **1992**, *25*, 6466.
(47) Meier, D. J. In *Block and Graft Copolymers*; Burke, J. J., Weiss, V., Eds.; Syracuse University Press: Syracuse, NY, 1973; Chapter 6.
(48) Van Krevelen, D. W. *Properties of Polymers: Their Estimation and Correlation with Chemical Structure*; Elsevier Scientific: Amsterdam, 1976; p 180.
(49) Datye, V. K.; Taylor, P. L. *Macromolecules* **1985**, *18*, 1479.
(50) Lefelar, J. A.; Weiss, R. A. *Macromolecules* **1984**, *17*, 1145.